

CONF-871234--3

CONF-871234--3

DE88 002898

## COMMIX ANALYSIS OF THE SODIUM HEATED HELICAL COIL STEAM GENERATOR

C. R. Kakarala  
Engineering Project Manager  
Babcock and Wilcox Company  
Barberton, Ohio

S. W. Burge  
Research Specialist  
Babcock and Wilcox Company  
Alliance, Ohio

W. T. Sha  
Director Analytical Thermal Hydraulic  
Research Program  
Argonne National Laboratory  
Argonne, Illinois

### DISCLAIMER

This report was prepared as an account of work sponsored by an agency of the United States Government. Neither the United States Government nor any agency thereof, nor any of their employees, makes any warranty, express or implied, or assumes any legal liability or responsibility for the accuracy, completeness, or usefulness of any information, apparatus, product, or process disclosed, or represents that its use would not infringe privately owned rights. Reference herein to any specific commercial product, process, or service by trade name, trademark, manufacturer, or otherwise does not necessarily constitute or imply its endorsement, recommendation, or favoring by the United States Government or any agency thereof. The views and opinions of authors expressed herein do not necessarily state or reflect those of the United States Government or any agency thereof.

The submitted manuscript has been authored by a contractor of the U. S. Government under contract No. W-31-109-ENG-38. Accordingly, the U. S. Government retains a nonexclusive, royalty-free license to publish or reproduce the published form of this contribution, or allow others to do so, for U. S. Government purposes.

MASTER

## ABSTRACT

This paper describes the COMMIX-HCSG computer program and compares predictions to data obtained from performance tests on a 76 Mwt Helical Coil Steam Generator (HCSG) test unit.

COMMIX-HCSG is a multi-dimensional thermal/hydraulic code that models both steady state and transient operation of an HCSG. The code solves a system of Navier-Stokes continuum equations that have been modified with a combination of volume and directional surface porosities and distributed resistances. This formulation properly accounts for the presence of tube bundle, supports, and baffles on the shell side of the steam generator. Turbulence models and heat transfer and pressure drop equations are used as applicable for the different regions including the upper plenum, the tube bundle, and the lower plenum of the HCSG.

The data was obtained from performance tests conducted in early 1987 on the 76 Mwt HCSG test unit at the Energy Technology Engineering Center (ETEC). The test unit contains over 700 instruments. HCSG development and tests are carried out as part of the Department of Energy program to develop reliable and economical liquid metal heated steam generators.

## NOMENCLATURE

C	=	specific heat
$g_r, g_\theta$	=	components of gravitational acceleration
$g_x, g_z$	=	in the r, theta, x and z directions.
h	=	fluid enthalpy
$K_{eff}$	=	effective thermal conductivity
P	=	fluid pressure
Q	=	volumetric heat source or sink
r	=	radial coordinate
$R_i$	=	distributed resistance component
$R_{Wi}$	=	thermal resistance between tube center and tubeside fluid
$R_{Wo}$	=	thermal resistance between tube center and shellside fluid
T	=	temperature
t	=	time

$u$	=	velocity in the r-direction or in the tubeside fluid
$V_w$	=	volume of tube material
$V_s$	=	$V_g - V_l$ , slip velocity
$v$	=	velocity in $\theta$ -direction
$w$	=	velocity in z-direction
$x$	=	coordinate in flow direction on tubeside
$z$	=	axial coordinate
$\alpha$	=	void fraction
$\gamma_j$	=	surface permeability component
$\gamma_v$	=	volumetric porosity
$\mu_{eff}$	=	effective viscosity
$\rho$	=	density
$\theta$	=	azimuthal coordinate

### Subscripts

$g$	=	vapor phase
$l$	=	liquid phase
$r$	=	r-direction
$s$	=	shell side
$t$	=	tube side
$w$	=	tube wall
$z$	=	z-direction
$\theta$	=	$\theta$ -direction

### INTRODUCTION

Detailed evaluations of local thermal/hydraulic conditions are very important in the design and development of reliable and economical advanced nuclear heat exchangers. These evaluations are needed for the entire range of expected operation including nominal as well as off-nominal conditions. Accurate thermal/hydraulic information is required for the predictions of the overall performance of the unit. It provides boundary conditions that are needed to assess the integrity and reliability of the design. For example, structural analyses often require local thermal/hydraulic conditions. To fulfill this need, multi-dimensional thermal/hydraulic codes are being developed and validated in recent years for various applications.

Reliability and safety of the sodium heated steam generators are of special concern in the liquid metal reactor plants because of the adverse effects of the potential sodium/water reactions. For these steam generators, the application of the multi-dimensional thermal/hydraulic (T/H) codes is particularly relevant because of the high temperature and large temperature gradients and the faster thermal transients associated with sodium. Because of their concerns, the U. S. Department of Energy has conducted an extensive development program on the sodium heated helical coil tube steam generator over the past 10 years. Reference [1] presented the results of the preliminary multidimensional T/H analysis of HCSG using a modified VARR-II code. As part of the DOE HCSG development program, a multi-dimensional T/H code called COMMIX-HCSG was modified from COMMIX IHX/SG [2] and was developed jointly by the Argonne National Laboratory and the Babcock and Wilcox Company [3,4].

The U. S. Department of Energy development program has also included an extensive test program on an HCSG prototype unit. A 76 Mwt Steam Generator was designed with extensive instrumentation and tested from July 1986 through February 1987.

This paper describes the COMMIX-HCSG code and compares predictions to data obtained from the performance tests. A description of the prototype, the instrumentation, and test program are also presented to provide a better understanding of the data and model comparisons.

#### TEST UNIT DESCRIPTION

The test unit is a one-sixth scale (76 Mwt) prototype of a plant size (438 Mwt) once-through helical coil tube steam generator. The schematic and dimensions of the test unit are given in Figure 1 and Table 1, respectively.

Table 1 - Design dimensions of the test unit

Tube outside diameter, mm	31.75
Tube minimum wall thickness, mm	4.32
Average tube length, m	110.30
Bundle height, m	7.61
Bundle longitudinal pitch, mm	47.60
Bundle transverse pitch, mm	50.80
Number of tubes	40
Number of coil rows	7
Heat transfer surface, m <sup>2</sup>	440.0
Unit height, m	17.49
Size of sodium inlet nozzles, mm	254.0
Size of sodium outlet nozzles, mm	305.0
Size of feedwater inlet nozzles, mm	152.0
Size of steam outlet nozzles, mm	152.0

Sodium enters at the top of the unit through a nozzle and is distributed by a central pipe distributor. Vanes on the bottom of the distributor direct the flow at an angle downward from the horizontal plane of the sodium level. Sodium level and argon cover gas space are maintained above the discharge of the sodium from the distributor to avoid gas entrainment and mitigate thermal stresses on the upper head components. Sodium flows downward and is redistributed uniformly in the radial direction by the helical coil tube bundle. The helical coil tube bundle is located between cylindrical inner and outer shrouds. The gaps between the tube bundle and shrouds are designed such that the sodium flow bypass

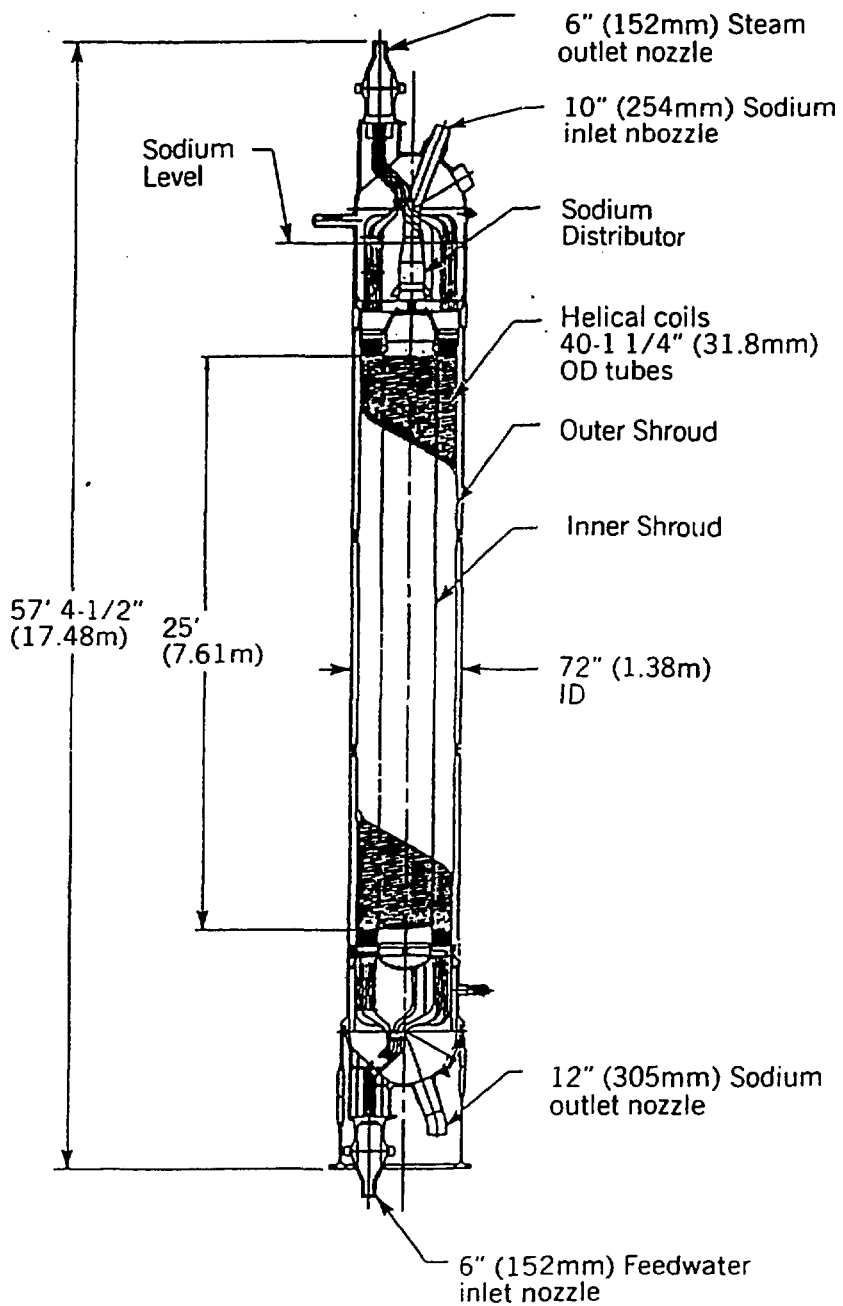


Figure 1 Helical coil steam generator 76 Mwt test unit

in the gaps will not be detrimental to the thermal and structural performance of the steam generator. At the bottom of the bundle, the sodium flow exits into the lower plenum, flows over the feedwater inlet tubes at low velocities and leaves the steam generator through a central nozzle on the bottom head.

Feedwater enters the steam generator through a tubesheet located on a non-radial feedwater nozzle on the bottom hemispherical head. The desired feedwater distribution to the tubes is achieved by attaching flow restrictors to the bottom face of the tubesheet at each tube hole. The restrictor resistance is varied as a function of the coil diameter of the tube. There are seven different tube coil rows with diameters ranging from 38 inches (0.96 m) to 62 inches (1.58 m) with a nominal gap between adjacent coil row tubes of 3/4 inches (19 mm) in the transverse direction to sodium flow. Water entering the tubes at the bottom tubesheet flows through the inlet tubes in the lower plenum, the helical coil tube bundle, the riser tubes in the upper plenum, and exits at the upper tubesheet as superheated steam for normal power operation.

## INSTRUMENTATION

The test unit is extensively instrumented with over 700 sensors including thermocouples (548), strain gages (109), accelerometers, flow, pressure drop and sodium level measuring devices. The helical coil tube bundle is instrumented with 145 thermocouples to fully characterize the heat transfer performance under a wide range of operating conditions. At one circumferential location, thermocouples are placed at 21 locations along the height of the tube bundle (thermocouple at each 5 percent increment of the bundle height) for three radial locations (between coil rows 1 and 2, 4 and 5, and 6 and 7). Several thermocouples are also located along the height of the bundle between the inner shroud and coil row 1 and between coil row 7 and the outer shroud to determine the degree of sodium bypass of the tube bundle for various operating conditions. Steam outlet temperatures of each of the 40 tubes were obtained by the thermocouples strapped to the tubes in the cover gas space region. Thermocouples are also placed at the steam outlet tubesheet directly in the steam flow path in seven tube outlets (one for each coil row). For the same tubes, feedwater inlet flow was obtained by measuring the pressure drop of the calibrated feedwater inlet restrictors. Steam outlet flow rate of the same tubes was also obtained by measuring pressure drop across venturies installed on the top face of the steam outlet tubesheet. Several thermocouples are also installed in the upper plenum to obtain the degree of sodium recirculation and heat transfer for various operating conditions. Feedwater inlet nozzle area is instrumented with 44 thermocouples to ascertain the thermal isolation of the feedwater tubesheet.

## TEST FACILITY

Tests were performed on the HCSG prototype test unit at the Sodium Component Test Installation (SCTI) of the Energy Technology Engineering Center (ETEC) near Los Angeles, California starting July 1986.

The SCTI facility is prototypic of a standard power plant. It includes a sodium heat transport system for delivering thermal energy to the test article, a steam and feedwater system for heat rejection and supporting auxiliary subsystems (e.g., electrical preheat, sodium purification, water purification, inert cover gas).

The plant includes special design features, such as low flow bypass lines and staged components, which are unique to a test facility and allow operation over an extremely wide range of conditions. Sodium inlet temperatures range from 204°C to 593°C with sodium flows up to  $1.81 \times 10^6$  kg/hr. The steam and feedwater system can provide water flows to the test article ranging from  $4.54 \times 10^3$  kg/hr to over  $5.0 \times 10^5$  kg/hr, with feedwater temperatures up to 316°C.

#### TEST PROGRAM

An extensive test program of about two years in duration is planned for the HCSG test unit. A broad range of tests including steady state, transient, upset, and emergency conditions will be performed.

The data from the tests will be used to assess the thermal/hydraulic and structural design margins, to verify design methods and correlations, and to validate the various design analysis thermal/hydraulic computer codes applicable to the HCSG. Initial steady state testing up to 50 percent

load has been completed. These test results are used here for data comparison with COMMIX.

## COMMIX HCSG MODEL AND ANALYSIS

In recent years, numerical methods have been developed and refined for solving complex multi-dimensional fluid flow problems [5,6]. Practical engineering tools have been developed with these methods and routinely used to study local as well as overall performance of heat exchanger components. For example, detailed operating conditions such as fluid velocity, temperature, void fraction, and heat flux profiles have been obtained in analyses of recirculating [7-13] and once-through [14-15] PWR steam generators and in analyses of LMFBR heat exchangers [2,16].

The multi-dimensional analyses reported here were performed with a version of the COMMIX-IHX/SG Code [2] that was modified to model the HCSG. The resulting program, denoted COMMIX-HCSG, contains the basic modeling approach of COMMIX-IHX/SG along with improvements and modifications that are considered important in modeling an HCSG. Because COMMIX-IHX/SG has been described earlier [2], only an overview of the code basics is given as it applies to COMMIX-HCSG. The features added to model the HCSG will be emphasized.

### Shell Side Model

The shell side, which contains the liquid sodium, is modeled three dimensionally in cylindrical coordinates. The continuum Navier-Stokes equations are modified [17,18] with a combination of volume and directional surface porosities and distributed resistances to account for obstructions in the flow field such as tubes, tube support plates, flow baffles, etc. This concept results in a proper accounting for fluid momentum as a result of area restrictions and allows for the use of correlations to approximate complex flow resistances in the flow field, such as the bundle by-pass flow model noted later. The shell side governing equations are:

#### Continuity equation.

$$\frac{\partial}{\partial t} [\gamma_v \rho] + \frac{1}{r} \frac{\partial}{\partial r} [\gamma_r \rho r u] + \frac{1}{r} \frac{\partial}{\partial \theta} [\gamma_\theta \rho v] + \frac{\partial}{\partial z} [\gamma_z \rho w] = 0 \quad (1)$$

Momentum equations.

$$\begin{aligned}
 & \frac{\partial}{\partial t} [\gamma_{\nu\rho u}] + \frac{1}{r} \frac{\partial}{\partial r} [\gamma_{r\rho r u^2}] + \frac{1}{r} \frac{\partial}{\partial \theta} [\gamma_{\theta\rho u v}] + \frac{\partial}{\partial z} [\gamma_{z\rho u w}] \\
 & - \frac{\gamma_{\theta\rho v^2}}{r} = -\gamma_{\nu} \frac{\partial p}{\partial r} - R_r + \frac{1}{r} \frac{\partial}{\partial r} \gamma_{r\mu\text{eff}r} \frac{\partial u}{\partial r} + \frac{1}{r^2} \frac{\partial}{\partial \theta} \\
 & \gamma_{\theta\mu\text{eff}} \frac{\partial u}{\partial \theta} + \frac{\partial}{\partial z} \gamma_{z\mu\text{eff}} \frac{\partial u}{\partial z} - \gamma_{r\mu\text{eff}} \frac{2}{r^2} \frac{\partial v}{\partial \theta} \\
 & - \gamma_{r\mu\text{eff}} \frac{u}{r^2} + \gamma_{\nu\rho g_r} \tag{2}
 \end{aligned}$$

$$\begin{aligned}
 & \frac{\partial}{\partial t} [\gamma_{\nu\rho v}] + \frac{1}{r} \frac{\partial}{\partial r} [\gamma_{r\rho r u v}] + \frac{1}{r} \frac{\partial}{\partial \theta} [\gamma_{\theta\rho v^2}] + \frac{\partial}{\partial z} \\
 & [\gamma_{z\rho v w}] + \frac{\gamma_{\nu\rho u v}}{r} = -\frac{\gamma_{\nu}}{r} \frac{\partial p}{\partial \theta} - R_{\theta} + \frac{1}{r} \frac{\partial}{\partial r} \gamma_{r\mu\text{eff}r} \frac{\partial v}{\partial r} \\
 & + \frac{1}{r^2} \frac{\partial}{\partial \theta} \gamma_{\theta\mu\text{eff}} \frac{\partial v}{\partial \theta} + \frac{\partial}{\partial z} \gamma_{z\mu\text{eff}} \frac{\partial v}{\partial z} + \gamma_{\theta\mu\text{eff}} \frac{2}{r^2} \frac{\partial u}{\partial \theta} \\
 & - \gamma_{\theta\mu\text{eff}} \frac{v}{r^2} + \gamma_{\nu\rho g_{\theta}} \tag{3}
 \end{aligned}$$

$$\begin{aligned}
 & \frac{\partial}{\partial t} [\gamma_{\nu\rho w}] + \frac{1}{r} \frac{\partial}{\partial r} [\gamma_{r\rho r u w}] + \frac{1}{r} \frac{\partial}{\partial \theta} [\gamma_{\theta\rho v w}] + \frac{\partial}{\partial z} \\
 & [\gamma_{z\rho w^2}] = -\gamma_{\nu} \frac{\partial p}{\partial z} - R_z + \frac{1}{r} \frac{\partial}{\partial r} \gamma_{r\mu\text{eff}r} \frac{\partial w}{\partial r} \\
 & + \frac{1}{r^2} \frac{\partial}{\partial \theta} \gamma_{\theta\mu\text{eff}} \frac{\partial w}{\partial \theta} \tag{4} \\
 & + \frac{\partial}{\partial z} \gamma_{z\mu\text{eff}} \frac{\partial w}{\partial z} + \gamma_{\nu\rho g_z}
 \end{aligned}$$

Energy equation.

$$\begin{aligned} & \frac{\partial}{\partial t} [\gamma_v \rho h] + \frac{1}{r} \frac{\partial}{\partial r} [\gamma_r \rho r u h] + \frac{1}{r} \frac{\partial}{\partial \theta} [\gamma_\theta \rho v h] \\ & + \frac{\partial}{\partial z} [\gamma_z \rho w h] = \frac{1}{r} \frac{\partial}{\partial r} \gamma_r r K_{eff} \frac{\partial T'}{\partial r} \\ & + \frac{1}{r^2} \frac{\partial}{\partial \theta} \gamma_\theta K_{eff} \frac{\partial T'}{\partial \theta} + \frac{\partial}{\partial z} \gamma_z K_{eff} \frac{\partial T'}{\partial z} + Q, \end{aligned} \quad (5)$$

where  $T'$  is the sodium temperature,  $\gamma_v$  the volume porosity,  $\gamma_i$  the directional surface porosity,  $R_i$  the distributed resistance component,  $Q$  the heat transferred from the shell side fluid to the tubes per unit volume. An effective viscosity and thermal conductivity,  $\mu_{eff}$  and  $K_{eff}$ , account for the effects of turbulence and are determined with a one-equation turbulence model [19].

Tube Side Model

On the tubeside, because the tube diameter is very small compared to its length, a one-dimensional model adequately describes the thermal hydraulics. The tubes are connected to common inlet and outlet plenums and can be modeled as either straight or helically coiled along their lengths. A two-phase, homogeneous equilibrium model, with an algebraic specification of velocity slip between the phases is used.

Continuity equation.

$$\frac{\partial \rho}{\partial t} + \frac{\partial}{\partial x} (\rho u) = 0 \quad (6)$$

Momentum equation.

$$\begin{aligned} & \frac{\partial [\rho u]}{\partial t} + \frac{\partial}{\partial x} [\rho u^2] = - \frac{\partial P}{\partial x} + \rho g_x - \frac{\partial F}{\partial x} \\ & - \frac{\partial}{\partial x} \frac{\alpha(1-\alpha)^{\rho_g \rho_l}}{\rho} V_s \cdot V_s \end{aligned} \quad (7)$$

Energy equation.

$$\frac{\partial [\rho h]}{\partial t} + \frac{\partial}{\partial x} [\rho u h] = \frac{T_w - T_t}{RW_i} \quad (8)$$

In the above,  $RW_i$  is the heat transfer resistance between the tube center and the tubeside fluid (water),  $\alpha$  the void fraction,  $\partial F/\partial x$  the frictional pressure drop, and  $V_s$  the slip velocity. All are determined by correlations for the HCSG given in Table 2. Expressions for the two phase fluid density, mass flux, and phasic velocities are given in [2].

Boundary conditions imposed in the model are:

- o Inlet temperature
- o Inlet or outlet pressure
- o Common inlet and outlet pressures to all tubes
- o Total water flow rate entering the unit

Water flow distribution that satisfies the total flow rate boundary condition is calculated at each time step.

### Tube Energy Equation

The shell side and tubeside fluids are thermally coupled by a tube energy balance:

$$V_w \rho_w C_w \frac{dT_w}{dt} = \frac{T_s - T_w}{R_{wo}} - \frac{T_w - T_t}{R_{wi}} \quad (9)$$

where  $R_{wo}$  is the heat transfer resistance between the tube center and the shell side fluid.

Implicit Continuum - fluid Eulerian (ICE) method [5] is used to develop finite difference equations and solution method for COMMIX-IHX/SG and COMMIX-HCSG. COMMIX-HCSG provides the following unique features:

### Implicit Solution Method

A MICE [20] (Modified Implicit Continuous - fluid Eulerian) type technique has been implemented. Using MICE, time steps larger than the Courant-Friedrichs-Lewy condition [21] can be taken and still maintain a stable solution. This method increases computational efficiency for long time transients that must be modeled by the HCSG designer.

### HCSG Correlations

The thermal hydraulic correlations in Table 2 have been implemented in COMMIX-HCSG.

Table 2 - Thermal/hydraulic correlations for the HCSG\*

Heat transfer correlations

Shell side sodium.

Tube bundle/oblique flow Kalish/Dwyer [24]

Upper and lower plenums/  
forced and natural convection Liquid metal  
handbook [25]

Tube side

Subcooled water Seban-McLaughlin  
[26]

Subcooled and nucleate boiling Chen [27]

Departure of nucleate boiling Carver/Kakarala/  
Slotnik [28]

Film boiling Ruffel [29]

Superheat Bishop [30]

Pressure drop correlations

Shell side frictional resistance Sha/Launders [19]

Tube side-single phase  
friction factor Mori/Nakayama  
[31]

Tube side-two phase  
void fraction, slip, and  
friction factor Thom [32]

\* For tube side, HCSG correlations were modified in some cases with Ito's [33] coil multiplier factor.

### Tube Configuration

As indicated above, a tube in the HCSG can be straight (head regions) or helically coiled (bundle region). Because the heat transfer and flow characteristics are affected by tube orientation and because tube location determines where heat transfer occurs to the shell side fluid, tube configuration along its length from the inlet to outlet plenums is considered in COMMIX-HCSG. This feature allows the designer to construct models of just the heads, just the bundle, or a single model with both regions.

### Vectored Inlet Flow Boundary Condition For The Sodium Distributor

A vectored inflow (inclined to the coordinate axes) [1] is used to model the inflow condition at the sodium distributor. The incoming flow is given both radial and axial velocity components that are imposed by distributor geometry. The inflow condition is important in predicting velocities and temperatures in the upper head which are boundary conditions for the bundle inlet.

### Shared Row Modeling

Figure 2 illustrates this model option in which a tube side control volume (part of a tube row) is located between two shell side volumes. Heat is transferred to both shell side volumes from the single, shared tube node. For the bundle region, this scheme results in shell side nodes being situated between tube rows where temperature measurements are made. In addition, the shroud to tube row bypass gap is better modeled with this scheme rather than with a node that includes the entire tube side volume adjacent to the shroud. It is noted that COMMIX-HCSG has the option to include an entire tube volume within a shell side node.

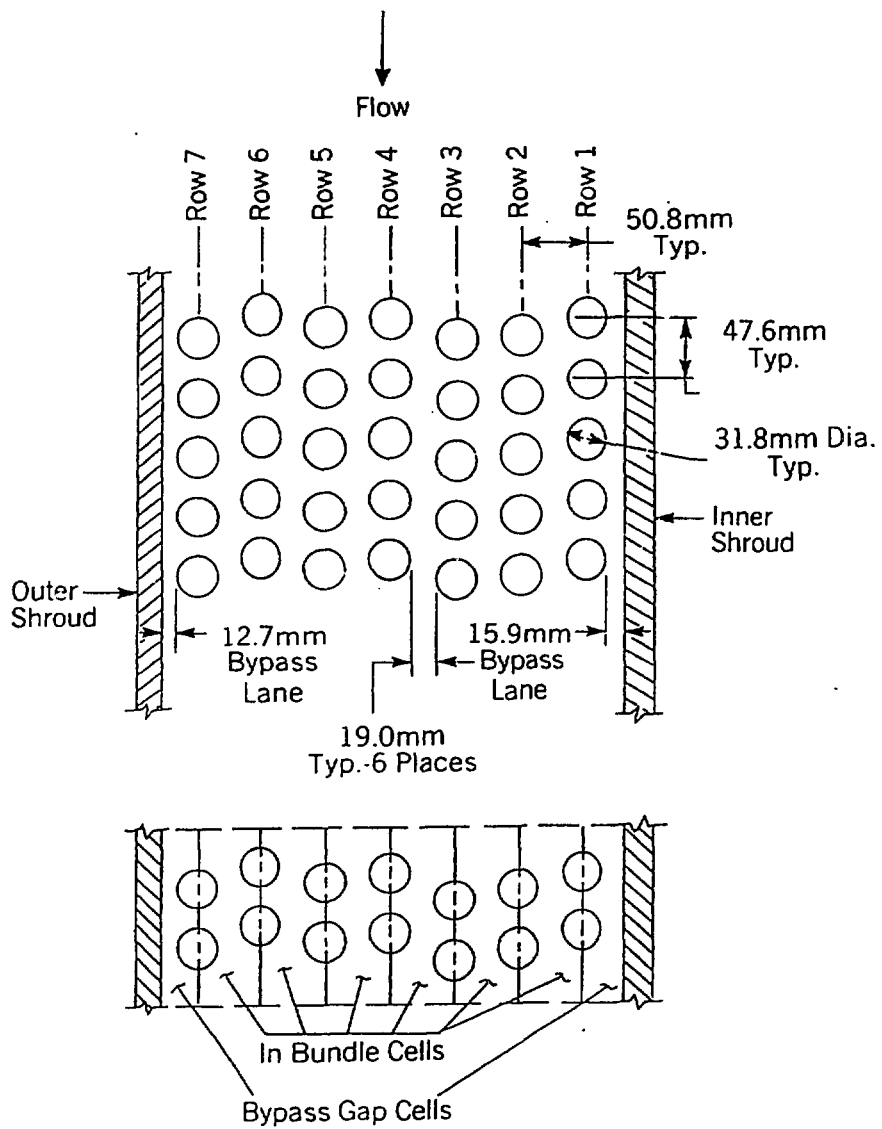


Figure 2 COMMIX tube bundle shared row modeling

### Bundle Bypass Flow Models

Bypass flow between the shrouds and bundle is a common concern in heat exchanger design. Two models [22, 23] for the flow resistance in the gaps are available as options in COMMIX-HCSG. The HTRI model [23] was specifically developed for the gap between the bundle and shroud. Jakob's model [22] was developed for fully developed flow in the tube bundle. However, it is applied here by assuming that the shroud is a symmetric plane adjacent to the edge tube row with the shroud providing no additional resistance. A two dimensional model, depicted in Figure 3, was used for all the analyses. A two, rather than three, dimensional model was initially formulated to minimize modeling complexity, to achieve a fairly detailed model that would execute in a reasonable time and to determine if test article performance could be adequately predicted with just a two-dimensional model. In this two-dimensional model, the upper head region is simulated with 13 radial and 28 axial control volumes, the bundle with 8 radial and 42 axial control volumes and the lower head with 16 radial and 9 axial control volumes. A total of 798 control volumes make up the model. This number appeared to be a good compromise between a fine discretization (many small control volumes) and a model that would execute in a reasonable time. Finally, unless otherwise noted, all analyses were performed with the HTRI [23] bypass model and the shared row modeling scheme.

### Water-Tube-Sodium Nodalization

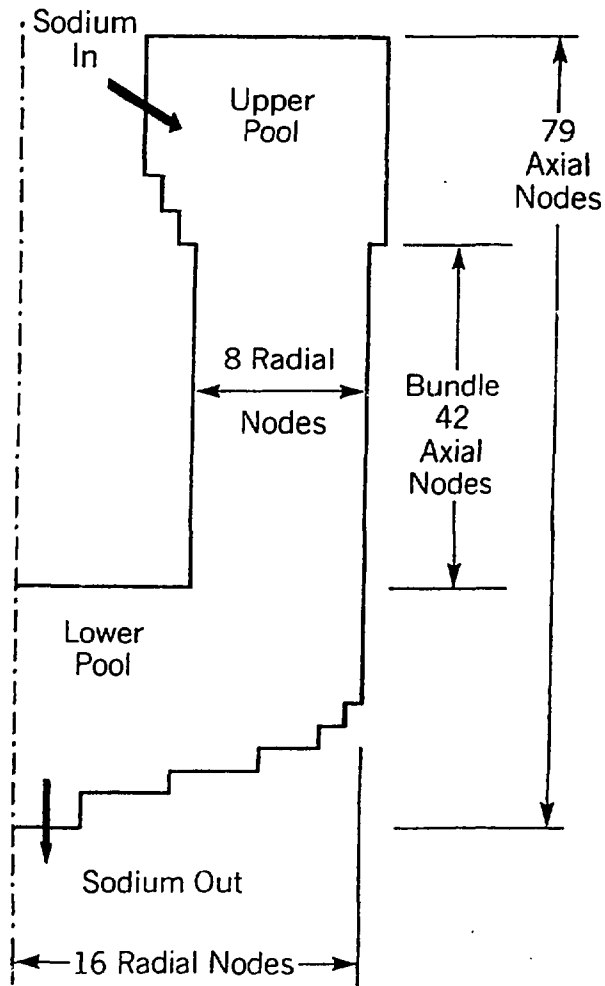


Figure 3 COMMIX steam generator model

## COMMIX-HCSG APPLICATIONS AND SCOPE OF DATA COMPARISONS

Multi-dimensional analysis is important in HCSG for both steady state and transient predictions [1]. However, the scope of data comparisons in this paper is limited to steady state performance applications, since initial tests this year were conducted only at steady state conditions up to 50 percent of the rated test unit thermal capacity. Multi-dimensional flow and heat transfer effects in two regions of the steam generator, tube bundle and upper head, are considered.

Under steady state condition, the thermal hydraulic performance of the bundle region is affected by the radial sodium and water flow distribution and the interaction effects of the heat transfer. A significant factor in this performance prediction is the amount of sodium flow rate in the bypass lanes. These lanes exist between the inner shroud and tube bundle, and the outer shroud and tube bundle. To illustrate the possible radial flow and temperature maldistribution effects, full load COMMIX-HCSG predictions of the test unit are given in Figures 4 and 5. Operating conditions are given in Table 3. Case 1 and Case 2 COMMIX predictions used the HTRI bypass flow resistance model [23] and Jacob's model [22], respectively. Design predictions on these figures were based on one dimensional

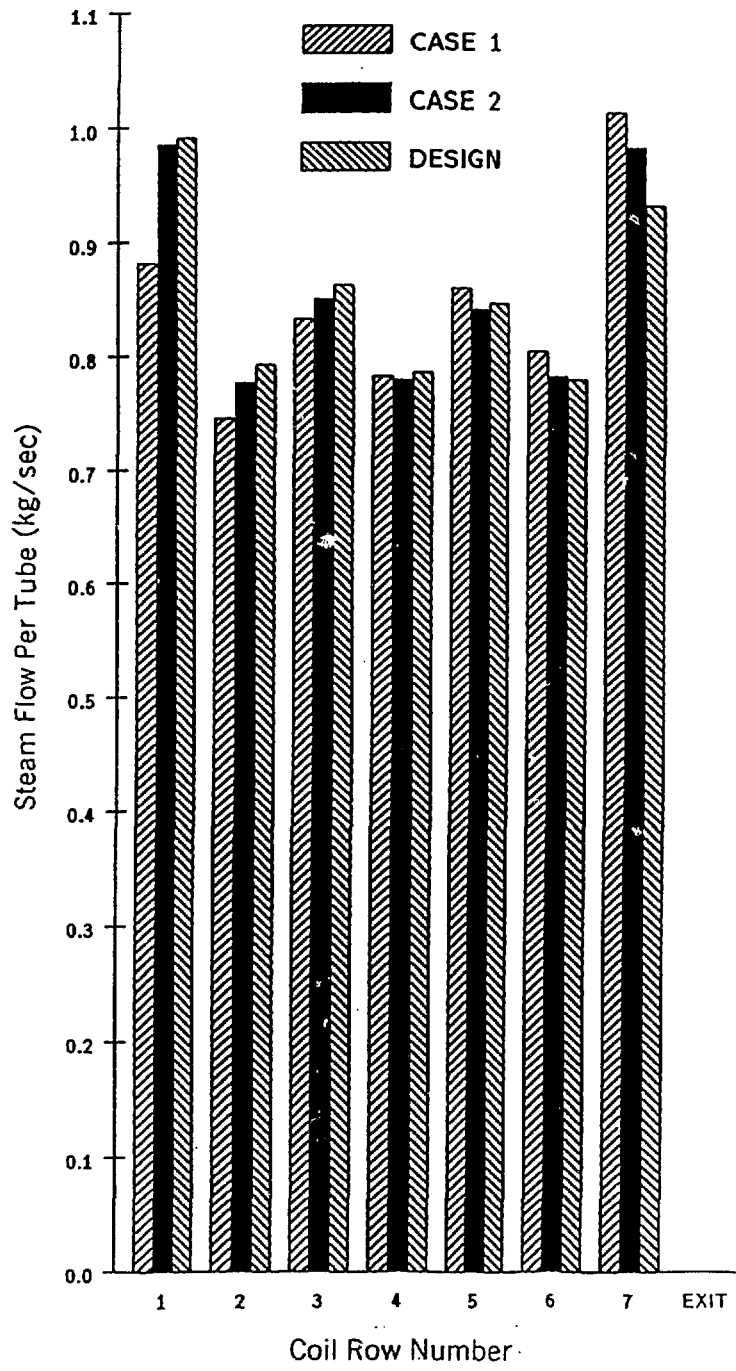


Figure 4 Water flow distribution predictions at full load

# Steam Temperature

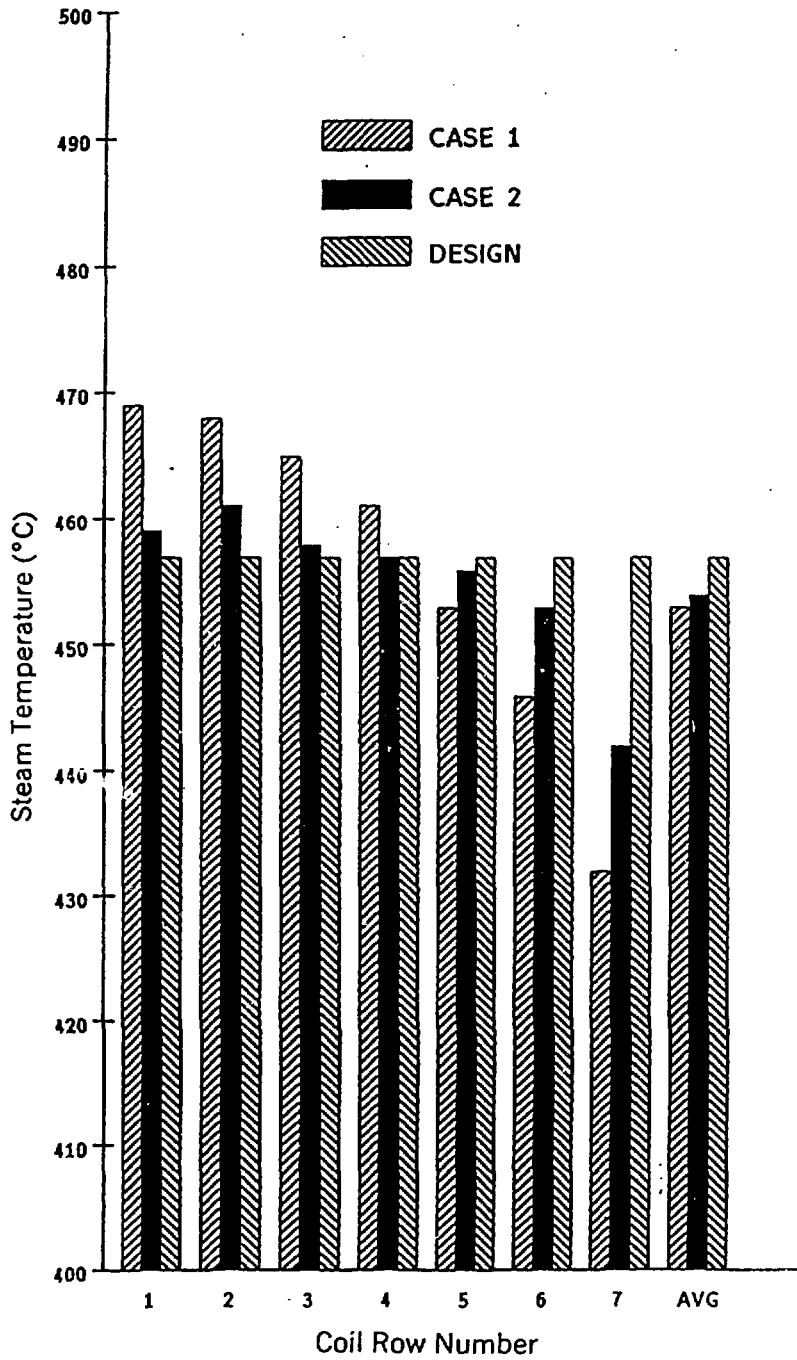


Figure 5 Steam outlet temperature distribution predictions at full load

Table 3 - Full load operating parameters of the test unit

Sodium inlet temperature, °C	482.0
Sodium outlet temperature, °C	316.0
Water inlet temperature, °C	216.0
Steam outlet pressure, MPa	15.67
Steam outlet temperature, °C	457.0
Sodium flow rate, kg/sec	368.70
Water flow rate, kg/sec	33.80
Unit capacity, MW <sub>t</sub>	76.0

performance analysis. These figures indicate that the multi-dimensional effects in the bundle can result in a prediction uncertainty of about 40°C in steam outlet temperature distribution. Predictions of bundle thermal hydraulic performance are compared to data for several operating conditions in the next section.

In the upper plenum of HCSG, sodium recirculation occurs due to the flow geometry and thermal buoyancy effects. These effects can be significant for operating conditions in which there is a large difference between the sodium inlet and steam outlet temperatures. A comparison of analysis and data is presented for a test run where these multi-dimensional effects significantly influence the heat transfer in the upper plenum.

## TEST RESULTS AND ANALYSIS

Predictions are compared to data from three test runs covering a range of sodium to water flow ratios. Run 1 had the nominal ratio of 11.4, Run 6 had the highest ratio of 18, and Run 8 had the lowest ratio of 8.

### Water Flow Distribution

Predicted and measured values of tube water flow are compared in Figures 6 to 8. The predictions include the variations in coil diameter, heat transfer lengths and pressure drops in the different heat transfer regimes. The predicted water flow rates are within 3 percent of the experimental data. This deviation is within the experimental uncertainty.

### Sodium Temperature Distribution

Measured sodium temperature profiles within the helical coil tube bundle are compared with the predictions for the inner (between Row 1 and Row 2), middle (between Row 4 and Row 5), and the outer (between Row 6 and Row 7) regions. These comparisons are shown in Figures 9 to 11. The measured temperatures are slightly higher than the predictions. Heat transfer lengths of the different heat transfer regimes on the water side change with the change in the sodium to water flow ratio. The shape and lengths of the predicted and measured temperature profiles for the three flow ratios are very similar. Sodium temperature profile predictions in the tube bundle bypass lanes were compared to the data for Run 1 in Figure 12. The predicted temperatures are slightly higher than the measured values which is opposite to that observed for the bundle sodium temperature comparisons shown in Figures 9 to 11. From these comparisons, it appears that the COMMIX-HCSG predictions with the HTRI bypass model have higher bypass flow rates than those indicated by the experimental data.

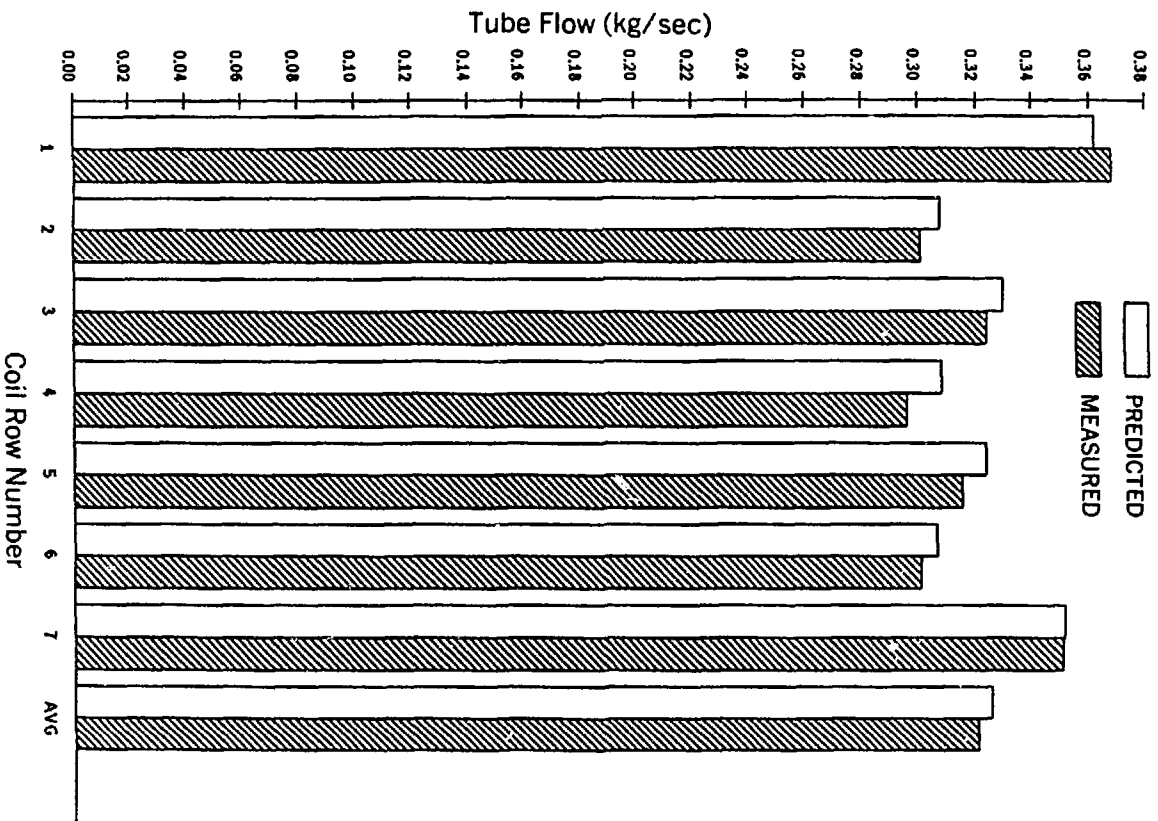


Figure 6 Water flow distribution comparisons at 40 percent load, test run no. 1

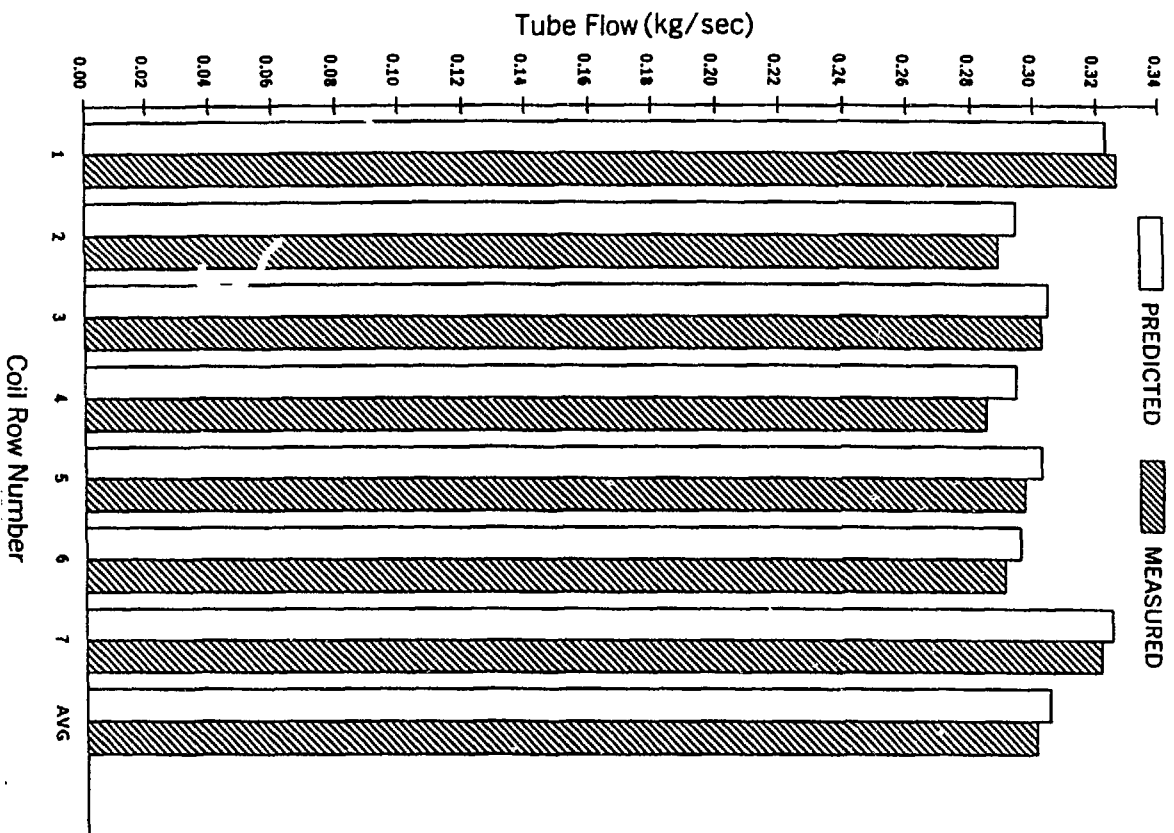


Figure 7 Water flow distribution comparisons at 40 percent load, test run no. 6

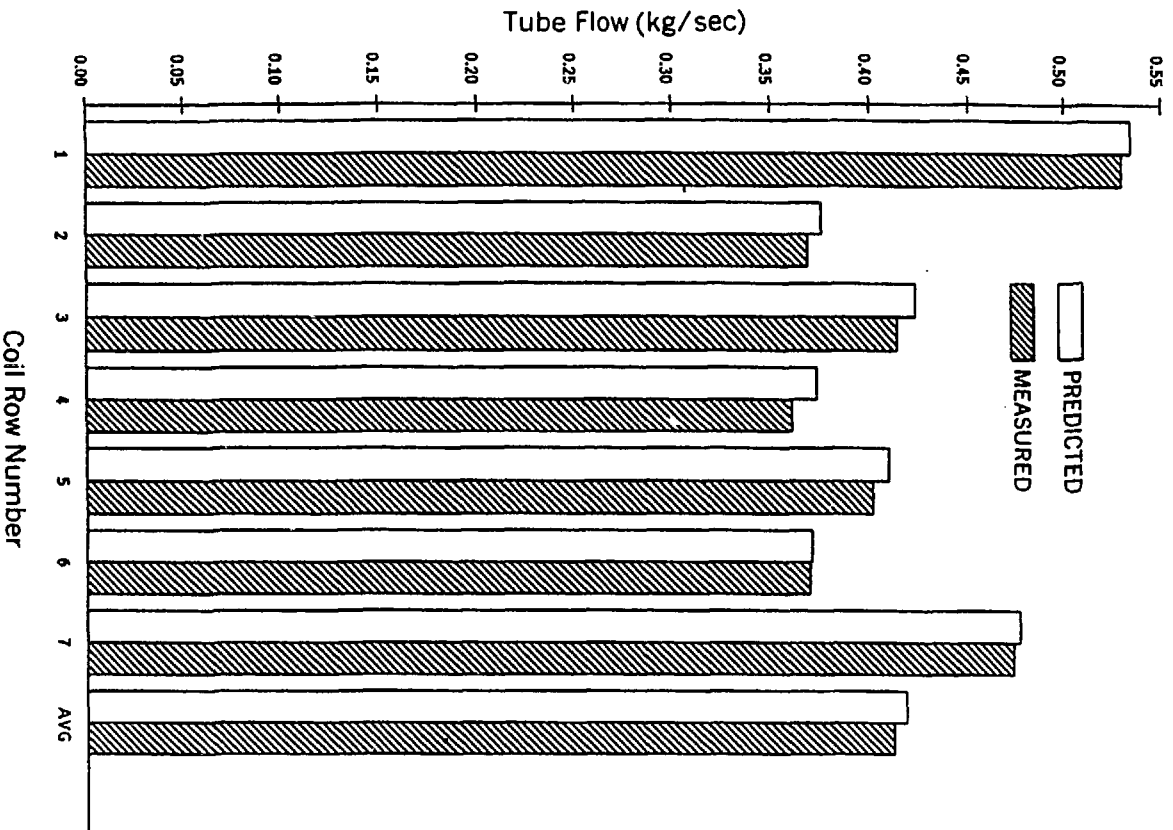


Figure 8 Water flow distribution comparisons at 40 percent load, test run no. 8

Sodium to Water Flow Ratio = 11.4,

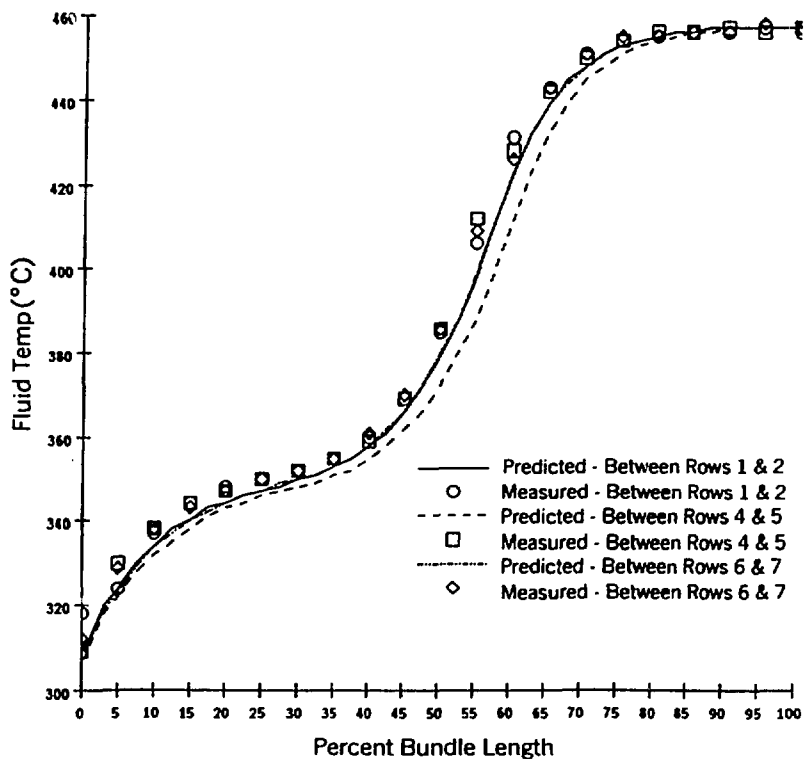


Figure 9 Sodium temperature profile in tube bundle comparisons, test run no. 1

Sodium to Water Flow Ratio = 18.0,

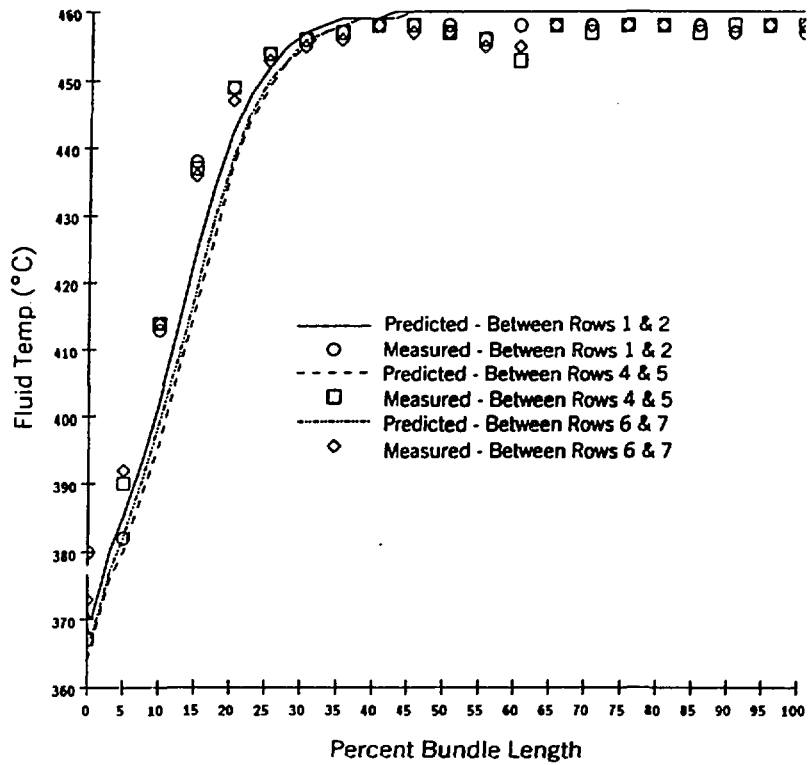


Figure 10 Sodium temperature profile in tube bundle comparisons, test run no. 6

**Sodium to Water Flow Ratio = 8.0**

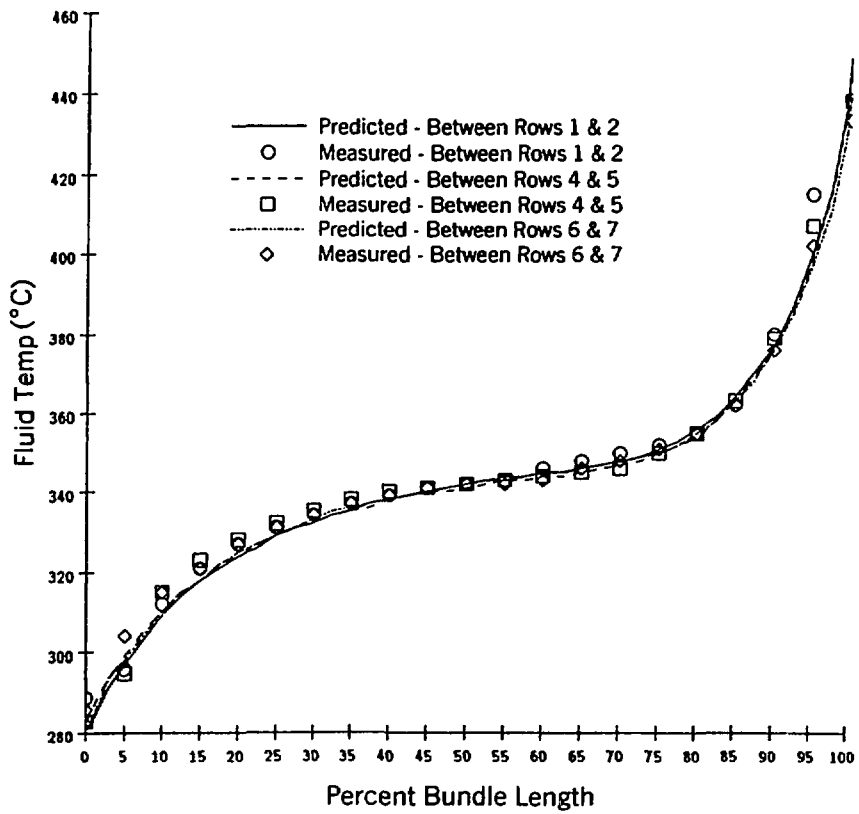


Figure 11 Sodium temperature profile comparisons in tube bundle, test run no. 8

**Sodium to Water Flow Ratio = 11.4**

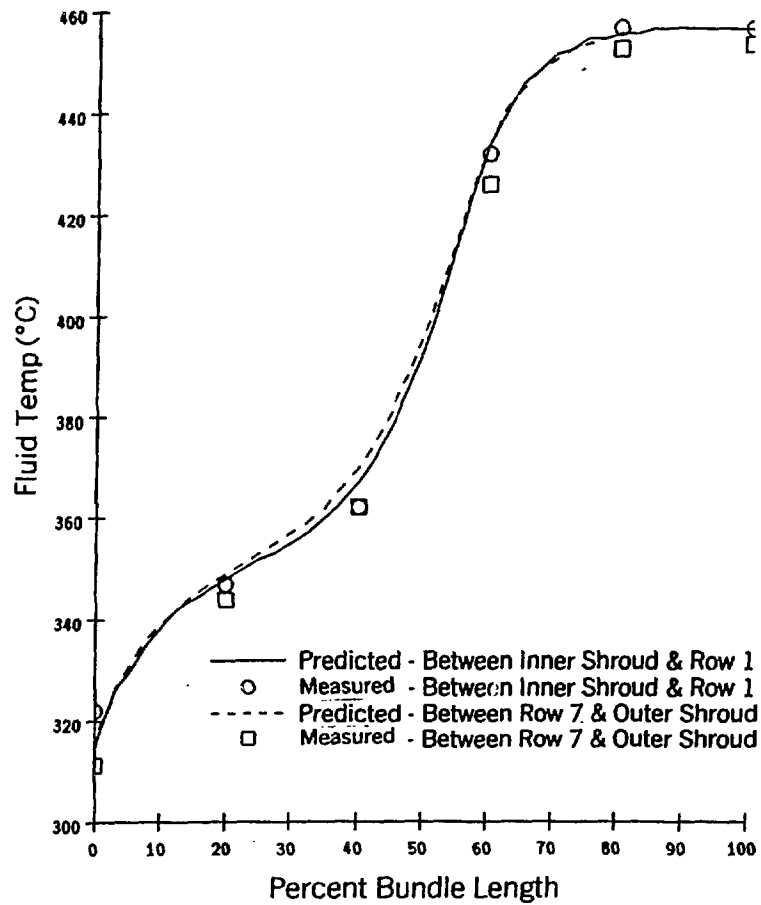


Figure 12 Sodium temperature profile comparisons near shrouds, test run no. 1

### Steam Outlet Temperature Distribution

Steam outlet temperatures of all the tubes for Run 1 and Run 6 are uniform and are essentially equal to the sodium inlet temperature. This is caused by the excess heat transfer surface in the steam generator for these operating conditions. However, for Run 8, with low sodium to water flow ratio, the steam outlet temperature is  $360.1^{\circ}\text{C}$  as compared to the sodium inlet temperature of  $459^{\circ}\text{C}$ . Because of this temperature difference, the predicted and measured steam outlet temperatures of the different coil row tubes, shown in Figure 13, exhibit some degree of non-uniformity. For the tubes in coil rows 1 and 7, the predicted steam outlet temperatures are higher than the data. In the interior of the tube bundle, the predicted steam outlet temperatures are lower than the measured values. These trends indicate that the predicted sodium bypass flow rate is higher than shown by the data. The effect of the sodium bypass is further illustrated by predicted sodium isotherms shown in Figure 14.

### Upper Plenum Sodium Temperature

A multidimensional sodium temperature distribution occurs in the upper plenum at operating conditions, such as Run 8, where there is a large sodium inlet to steam outlet temperature difference. The thermal/hydraulic operating conditions can therefore only be evaluated with a multidimensional model such as COMMIX-HCSG. Figure 15 shows the predicted sodium velocity distribution in the upper plenum. The length of the vectors indicate the magnitude of the velocity and their orientation the direction of the flow. Sodium recirculation shown in this plot influences the upper plenum sodium temperatures and heat transfer. Figure 16 shows the predicted isotherms along with experimental data in the upper plenum. Good agreement is seen for the sodium temperatures approaching the tube bundle. Predictions of these temperatures must include the multi-dimensional effects (flow and temperature) between the sodium distributor and bundle inlet.

Above the discharge of the distributor, the measured data shows significantly higher sodium temperatures than those predicted by COMMIX. Although COMMIX is predicting multi-dimensional flow and temperature conditions, the code is under estimating the amount of recirculation above the distributor. The under prediction of recirculation is caused by deficiencies in the turbulence model and in the sodium distributor boundary condition.

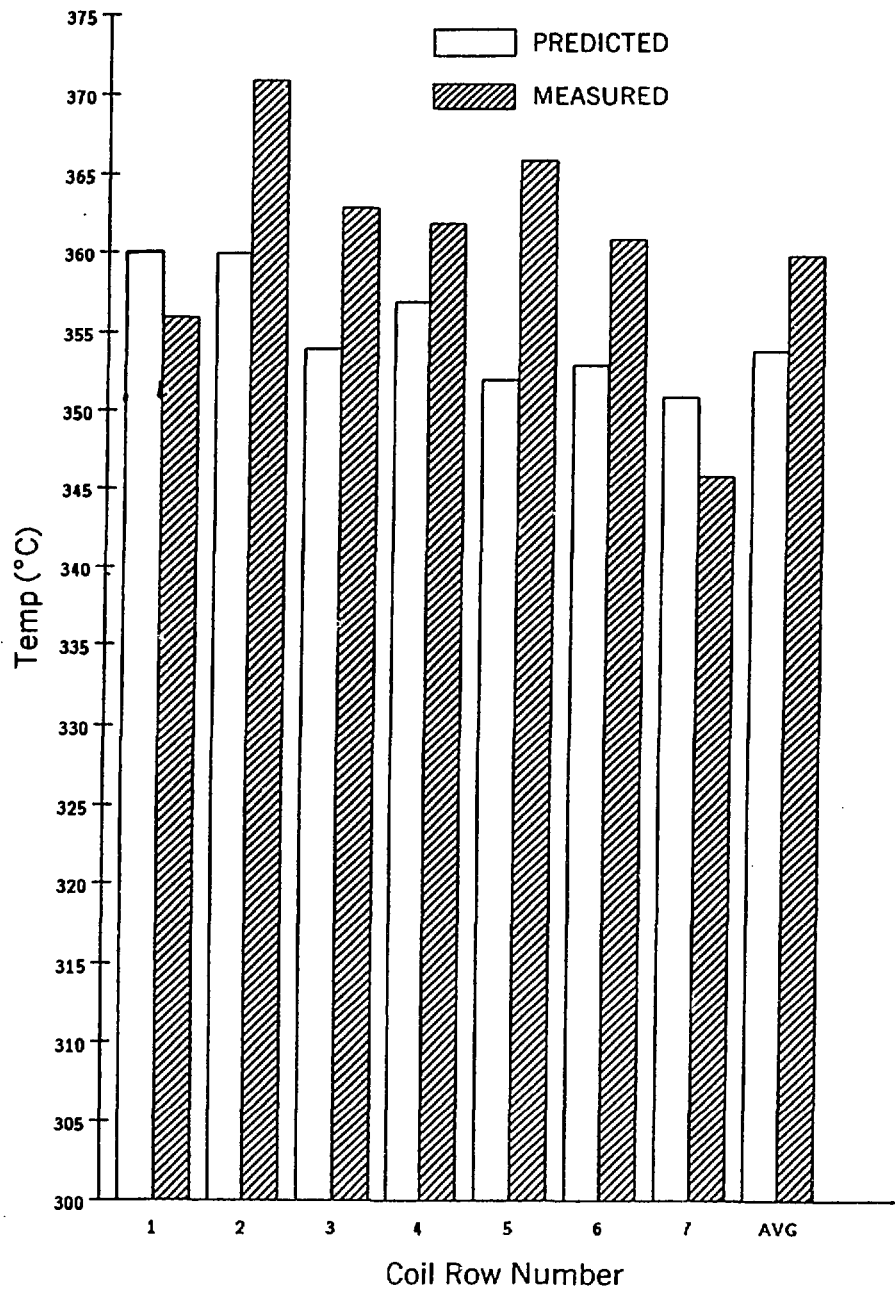


Figure 13 Steam outlet temperature distribution comparisons, test run no. 8

Contour Spacing is 10.00 Deg. C.

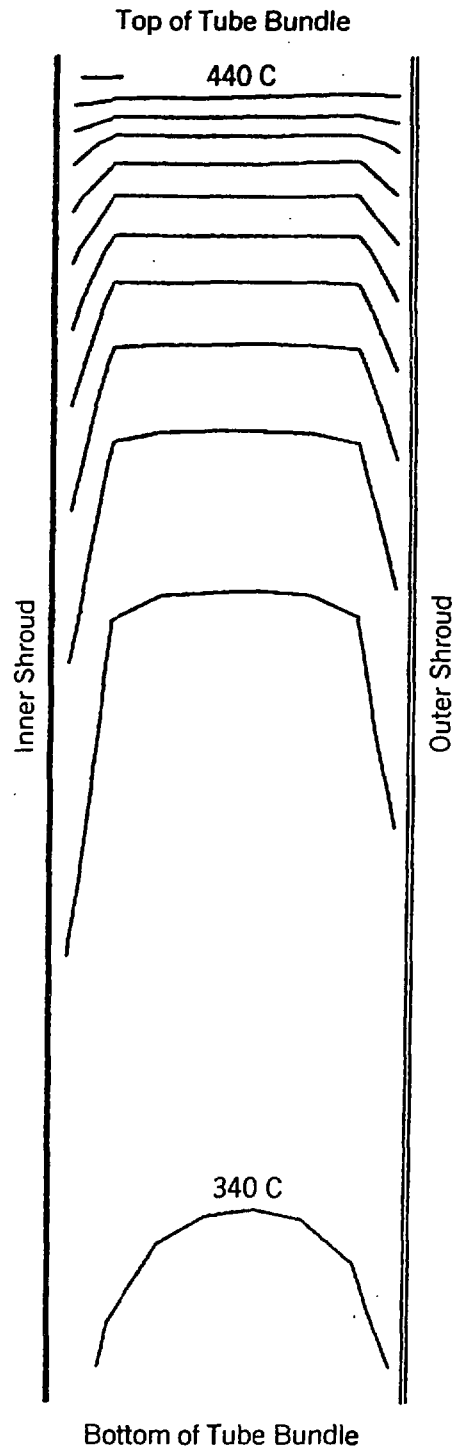


Figure 14 Contour plot of sodium temperature profiles in tube bundle

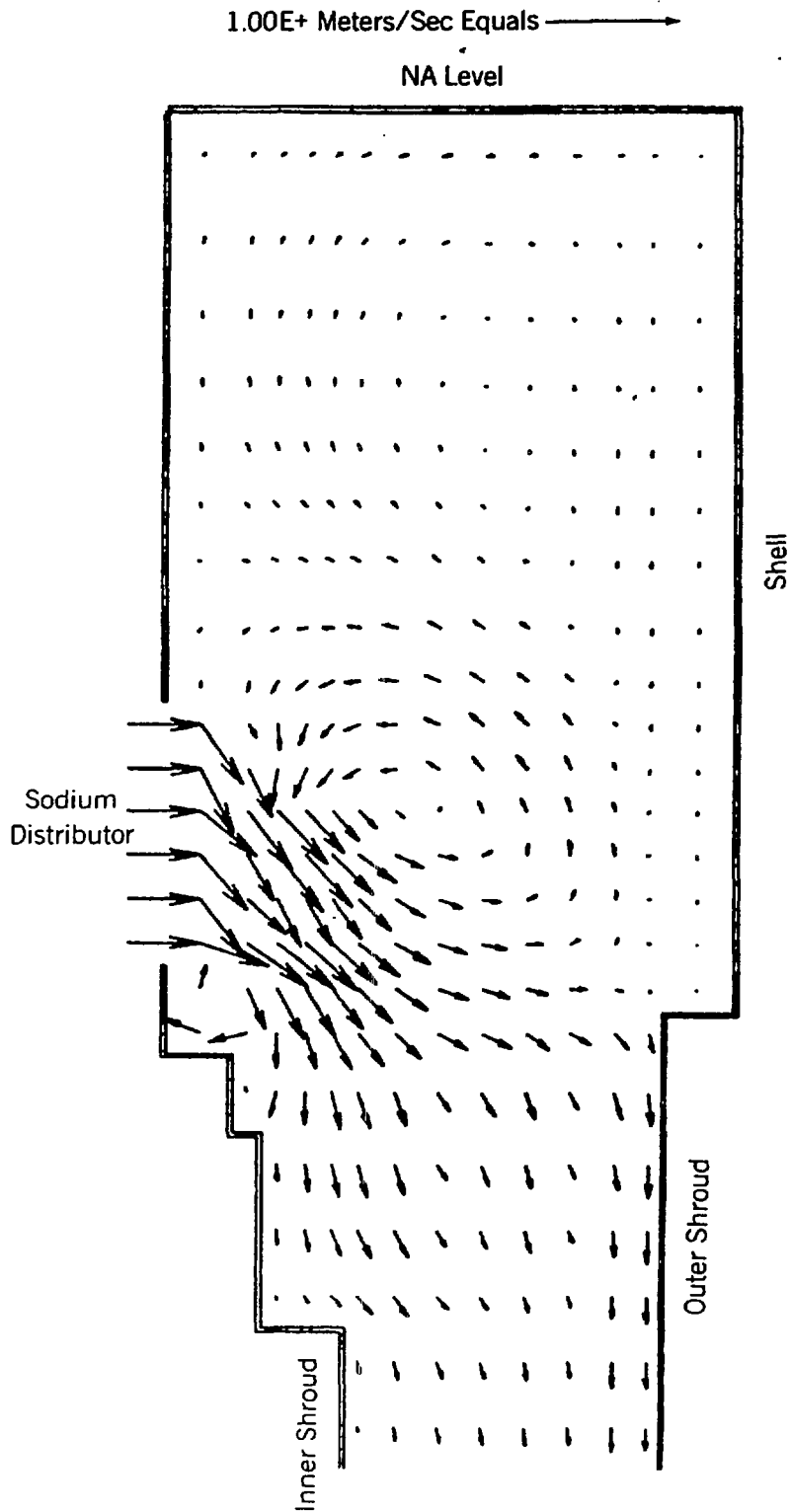


Figure 15 Sodium velocity vector plot in upper plenum near distributor

Contour Spacing is 5.000 Deg. C.

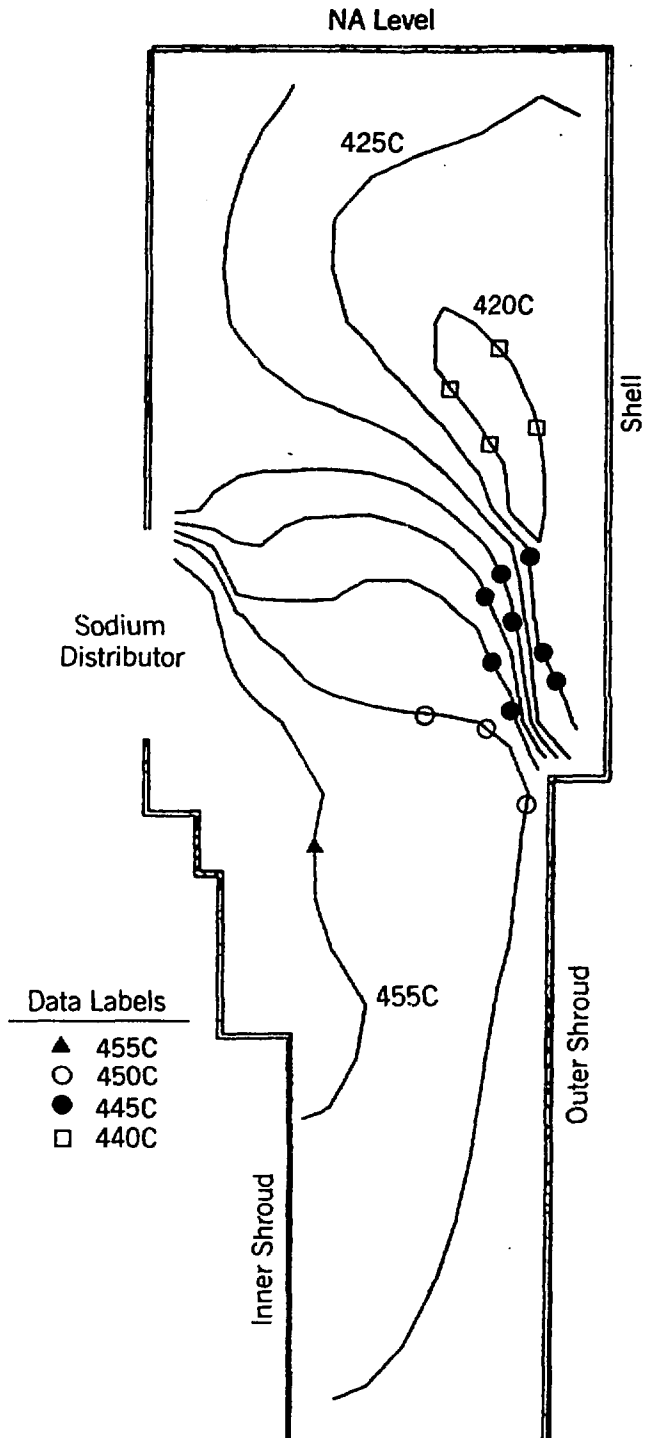


Figure 16 Sodium temperature profiles in the upper plenum

## CONCLUSIONS

1. A computer program, COMMIX-HCSG, has been developed to model the multi-dimensional thermal hydraulic performance of a helical coil tube steam generator. It includes features important to modeling a HCSG and can simulate both steady state and transient operation of the unit.
2. COMMIX-HCSG predictions agree very well with initial steady state data taken on the 76 Mwt helical coil tube test unit.
3. Some deficiencies in the empirical flow resistance correlations, turbulence model, and distributor boundary condition are identified. Further refinement and validation with a wider range of test data are planned.

## ACKNOWLEDGEMENT

The authors wish to thank all members of the Analytical Thermal Hydraulic Research Program Teams at the Argonne National Laboratory and the Babcock and Wilcox Company. This paper is based on work which was supported by the U.S. Department of Energy under ANL Contract and the Babcock and Wilcox Company Contract Number 610-0231.

## REFERENCES

1. Smith, D.C., Gerhart, P.M., and Kakarala, C.R., "Preliminary Multidimensional Thermal-Hydraulic Analysis of a Helical Coil LMFBR Steam Generator", ANS Transactions, Vol.44, June 1983, pp 596-597.
2. Sha, W.T., Kao, T.T., Yang, C.I. and Cho, S.M., "Multidimensional Numerical Modeling of Heat Exchangers", Journal of Heat Transfer, Trans. ASME, Vol. 104, August 1982, PP 417-425.
3. Yang, C.I., Kuzanek, J.F., Sha, W.T., Burge, S.W., and Kakarala, C.R., private communication.
4. Yang, C.I., Kuzanek, J.F., Sha, W.T., Burge, S.W., and Kakarala, C.R., private communication.
5. Harlow, F.H. and Amsden, A.A. "A Numerical Fluid Dynamics Calculation Method for All Flow Speeds", Journal of Computational Physics, Vol.8, No.2, 197-213, October 1976.
6. Patankar, S.V., Numerical Heat Transfer and Fluid Flow, Hemisphere Publishing Corp., Washington, DC 1980.
7. Lee, A.Y., Masiello, P.J. and Steininger, D.A., "Comparison of ATHOS Predictions of Tube Bundle Cross Flow Velocity With Experimental Data", ASME Paper 86-WA/NE-2, December, 1986.
8. Keeton, L.W., Habchi, S.D., Singhal, A.K., and Srikantiah, G.S., "Thermal Hydraulic Analysis/ Data Comparison of Two U-Tube Steam Generators Using the ATHOS 3 Code", ASME Paper 86-WA/NE-1, December, 1986.
9. Pettigrew, M.J., Carlucci, L.H., Ko, P.L., and Holloway, G.L., "Computer Techniques to Analyse Shell-and-Tube Heat Exchangers", ASME Paper 83-HT-61, 1983.

10. Inch, W.W.R. and Shill, R.H., "Thermal-Hydraulics of Nuclear Steam Generators: Analysis and Parameter Study", ASME Paper 80-C2 /NE-7, 1980.
11. Masiello, P.J., "Thermal-Hydraulic Code Qualification: ATHOS 2 and Data from Buget 4 and Tricastin", EPRI Report NP-2872, February 1983.
12. Inch, W.W.R., "Thermal-Hydraulic Analysis of Combustion Engineering Series 67 Steam Generator", EPRI Report NP-1678, January 1981.
13. Fortino, R.T., Rice, J.G., Oberjohn, W.J. Wang, J.H., and Cornelius, D.K., "Theda-2: A Multidimensional Steam Generator Thermal-Hydraulic Model", EPRI Report NP-3031-CCM, December 1983.
14. Keeton, L.W., Singhal, A.K., "ATHOS3 Code Analysis of Tube Plugging Effects on the Thermal-hydraulic Characteristics of a Once-Through Steam Generator", ASME Paper 86-WA/NE-4, December 1986.
15. Oberjohn, W.J., and Fortino, R.T., "A Multi-Dimensional Thermal-Hydraulic Analysis of Nuclear Once-Through Steam Generators", ASME Paper 82-FE-7, 1982.
16. Mes, H., Van Essen, D., Kirkcalby, D., and Phelps, P.J., "PHOENICS Code Thermal Hydraulic Analysis of a Prototype LMFBR Straight Tube Steam Generator", ASME Paper 86-WA/NE-5, December 1986.
17. Sha, W.T., "An Overview Of Rod Bundle Thermal-Hydraulic Analysis", Argonne National Laboratory, Report No. NUREG/CR-1825, ANL-79-10, November, 1980.
18. Sha, W.T., Domanus, H.M., Schmitt, R.C., Oras, J.J., and Lin, E.I.H., "COMMIX-1: A Three Dimensional Transient Single Phase Component Computer Program for Thermal Hydraulic Analysis", Argonne National Laboratory Report, NUREQ/CR-0785, ANL-77-96, September, 1978.
19. Sha, W.T., and Launder, B.E., private communication.

20. Bulgarelli, V., Casulli, V., and Greenspan, D., "Pressure Method for the Approximate Solution of the Navier-Stokes Equations", Numerical Methods in Laminar and Turbulent Flow, Ed. by Taylor, C., Johnson, J.A., Smith, W.R., Pineridge Press, 1983.
21. Courant, R., Friedrichs, K.O., Lewy, H., Math. Am. 100, 32 1928 (English Translation) IBM J. Res. Devel. 11, 215-234, 1967.
22. Jakob, M., "Heat Transfer and Flow Resistance in Cross Flow of Gases Over Tube Banks", Trans. ASME, Vol. 60, 384-386, 1938.
23. Palen, J.W., Taborek, J., and Yarden, A., "Stream Analysis Method for Prediction of Shell-side Heat Transfer and Pressure Drop in Segmentally Baffled Exchangers" Heat Transfer Research, Inc. Report 5-55-3-1, 1977.

24. Kalish, S. and Dwyer, O., "Heat Transfer to NaK Flowing Through Unbaffled Rod Bundles," Int. Journal of Heat Mass Transfer, Vol. 10, 1967, pp. 1533-1558.
25. Foust, O., ed., Sodium NaK Engineering Handbook, Gordon and Breach, Science Publishers, Inc., New York, 1976.
26. Seban, R. and McLaughlin, E., "Heat Transfer in Tube Coils with Laminar and Turbulent Flow," Int. Journal of Heat Mass Transfer, Vol. 6, 1963, pp. 387-395.
27. Chen, J. C., "A Correlation for Boiling Heat Transfer to Saturated Fluids in Convective Flow," ASME 63-HT-34.
28. Carver, J. R., Kakarala, C. R., and Slotnik, J.S., "Heat Transfer in Coiled Tubes with Two-Phase Flow," TID 20983, 1964.
29. Ruffell, A. E., "The Application of Heat Transfer and Pressure Drop Data to the Design of Helical Coil Once-Through Boilers," Multi-Phase Flow Systems, Institution of Chemical Engineers Symposium Series No. 38, Vol. II, BL 104.
30. Bishop A., Krambeck, F., and Sandberg, R., "Forced Convection Heat Transfer to Superheated Steam at High pressure and High Prandtl Numbers", ASME 65-WA/HT-35.
31. Mori, Y. and Nakayama, W., "Study on Forced Convection Heat Transfer in Curved Pipes (2nd Report, Turbulent Region)," Int. Journal of Heat Mass Transfer, Vol. 10, 1967, pp. 37-59.
32. Thom, J. R. S., "Prediction of Pressure Drop During Forced Circulation Boiling of Water," Int. Journal of Heat Mass Transfer, Vol. 7, 1964, pp 709-724.
33. Ito, J., "Friction Factors for Turbulent Flow in Curved Pipes," Journal of Basic Engineering, Vol. 81, June 1959, pp. 123-134.